

The Multiscale Maximum Change Algorithm for Subsurface Characterization

Abdullah Al Mamun[1], Alsadig Ali[1], Abdullah Al-Mamun[2], Felipe Pereira[1], and Arunasalam Rahunanthan[3(✉)]

[1] Department of Mathematical Sciences, The University of Texas at Dallas, Richardson, TX 75080, USA
[2] Institute of Natural Sciences, United International University, Dhaka, Bangladesh
[3] Department of Mathematics and Computer Science, Central State University, Wilberforce, OH 45384, USA
aRahunanthan@centralstate.edu

Abstract. The characterization of subsurface formations is a formidable task due to the high dimension of the stochastic space involved in the solution of inverse problems. To make the task computationally manageable, one needs to apply a dimensional reduction technique. In this paper we are considering the Karhunen Loève expansion (KLE) as the aforementioned technique. Considering the subsurface properties of interest, such as permeability and porosity, it may be suitable to localize the sampling method so that it can better accommodate the large variation in rock properties. In a Bayesian framework we investigate the solution of an inverse problem involving an elliptic partial differential equation for porous media flows. We propose a new multiscale sampling algorithm in which the prior distribution is expressed in terms of local KL expansions in non-overlapping subdomains of the domain of the inverse problem. We solve the inverse problem using multiple Markov Chain Monte Carlo (MCMC) simulations performed on a multi-GPU cluster. The simulation results indicate that the proposed algorithm significantly improves the convergence of a preconditioned MCMC method.

Keywords: Preconditioned MCMC · MCMC convergence · Inverse Problem · Multiscale Sampling · Domain Decomposition

1 Introduction

It is of great economic importance to find solutions to large scale inverse problems in geophysics [33] and petroleum engineering [1]. To find the solutions to these problems, we first need to numerically solve the partial differential equations that are used to mathematically model the problem. Then, in a Bayesian statistical framework, we simulate the numerical solver repeatedly to solve the inverse problem [2,11,15,23].

Multiscale numerical solvers have been quite successful in producing computationally inexpensive, accurate numerical solutions in porous media applications [10,16,18]. These methods are based on a domain decomposition

© The Author(s), under exclusive license to Springer Nature Switzerland AG 2023
O. Gervasi et al. (Eds.): ICCSA 2023 Workshops, LNCS 14105, pp. 114–129, 2023.
https://doi.org/10.1007/978-3-031-37108-0_8

technique [28]: local solutions computed at subdomains are combined to construct the global solution.

In the context of uncertainty quantification problems in [20] a domain decomposition approach was used for uncertainty analysis of PDEs. In this approach the authors independently performed the analysis on each local component offline and assembled the global uncertainty analysis using the precomputed local information. An efficient method to solve large scale KL decomposition problems was presented in [7]. In this method, the computational domain is divided into nonoverlapping subdomains, and on each subdomain a KL decomposition problem is solved to generate local bases. The local bases are used to discretize the global modes over the entire domain.

We investigate the application Markov Chain Monte Carlo methods to solve large inverse problems in the area of multiphase flows in porous media. The MCMC methods are known to converge slowly to the stationary distribution and we developed methods to speedup the convergence of these methods. In the Multiscale Sampling Method (MSM) [3,4] we combined local KL expansions with a new local averaging technique to improve drastically the convergence rates of the preconditioned MCMC method of [6,9]. The MSM algorithm consists of two steps: a global search in all the subdomains of the domain of the problem and a local search within each subdomain. In the work reported here we present a new development of this two step algorithm. We use the first step of the MSM to select the subdomain that shows the best acceptance of MCMC proposals and the second step of the MSM algorithm is modified to perform the search in the selected subdomain in the first step. Our simulation results show improved convergence of the new algorithm in comparison to the previous MSM.

The paper is organized as follows. In Sect. 2, we start by outlining the governing equations for pollutant transport in a porous medium. A Bayesian framework for subsurface characterization and KLE to reduce the dimension of the stochastic space are presented in Sect. 3. We also present the convergent assessments of the MCMC methods in Sect. 4. The simulation results are presented in Sect. 5. Section 6 is dedicated to provide conclusions of the study.

2 Model Problem

Let us consider a mathematical model that describes the subsurface transport of pollutants in a heterogeneous permeability field. In this model, the system of governing equations consists of an elliptic equation coupled with a hyperbolic equation. The elliptic equation is given by

$$\begin{cases} \boldsymbol{u} & = -k(\boldsymbol{x})\nabla p \qquad \text{in } \Omega \\ \nabla \cdot \boldsymbol{u} & = f \qquad\qquad\ \ \text{in } \Omega, \end{cases} \tag{1}$$

where $\Omega \subset \mathbb{R}^2$ is a bounded domain with a Lipschitz boundary $\partial\Omega$, $\boldsymbol{u}$ is the Darcy velocity, p represents the fluid pressure, $k(\boldsymbol{x})$ is a positive definite tensor also known as the absolute permeability field of the rock and $f \in L^2(\Omega)$ denotes

the sources and the sinks. Note that the typical boundary conditions for porous media flow problems are Dirichlet and Neumann and in this case the pressure and the normal component of the velocity is defined by

$$p = g_p \in H^{\frac{1}{2}}(\partial\Omega_p), \qquad \boldsymbol{u} \cdot \hat{\boldsymbol{n}} = g_{\boldsymbol{u}} \in H^{-\frac{1}{2}}(\partial\Omega_{\boldsymbol{u}}),$$

where $\partial\Omega = \overline{\partial\Omega_p} \cup \overline{\partial\Omega_{\boldsymbol{u}}}$, $\overline{\partial\Omega_p} \cap \overline{\partial\Omega_{\boldsymbol{u}}} = \varnothing$ and $\hat{\boldsymbol{n}}$ is the outward unit normal vector. The weak formulation of the pressure-velocity equation is used to derive the numerical approximation of the elliptic equation given by Eq. (1). Refer [10] for the weak formulation.

The hyperbolic equation is given by

$$\phi(\boldsymbol{x})\frac{\partial s(\boldsymbol{x},t)}{\partial t} + \nabla \cdot [s(\boldsymbol{x},t)\boldsymbol{u}(\boldsymbol{x})] = 0, \tag{2}$$

where $\phi(\boldsymbol{x})$ represents the rock porosity and $s(\boldsymbol{x},t)$ is the pollutant concentration in the water.

The aquifer contains spill and monitoring wells. To characterize the permeability field of the domain we use fractional flow data defined by

$$F(t) = 1 - \frac{\int_{\partial\Omega_{\text{out}}} u_n(\boldsymbol{x}) s(\boldsymbol{x},t)\ dl}{\int_{\partial\Omega_{\text{out}}} u_n(\boldsymbol{x})\ dl},$$

where $\partial\Omega_{\text{out}}$ is the well outflow boundary and $u_n(\boldsymbol{x})$ is the normal components of the velocity field [26]. In this paper, we consider only the elliptic equation Eq. (1) to demonstrate the significance of the proposed algorithm.

3 Characterization of Subsurface

3.1 The Bayesian Framework

The focus of this study is to characterize the permeability field using the available pressure data on the domain of the problem. We take that the pressure measurements are available on all the black (or white) squares on a chess board. That is, we have the measurements on one half of the discretized domain [34]. The characterization is done in a Bayesian statistical framework, which consists a preconditioned MCMC method. The preconditioned MCMC method will be discussed in Sect. 4.3.

Let us use $\boldsymbol{\eta}$ and R_p, respectively, for the (log of the) permeability field and the pressure measurement data. Using the Bayes' theorem, the posterior probability for the pressure data R_p can be written by

$$P(\boldsymbol{\eta}|R_p) \propto P(R_p|\boldsymbol{\eta})P(\boldsymbol{\eta}), \tag{3}$$

where $P(\boldsymbol{\eta})$ is a Gaussian prior distribution. The normalizing constant is not required for an MCMC algorithm and is therefore ignored. We use KLE to construct the (log of) permeability field $\boldsymbol{\eta}(\boldsymbol{\theta})$ and the MCMC algorithm is used

to generate the chain of $\boldsymbol{\theta}$s. KLE will be discussed in Sect. 3.2. A likelihood function for our problem, which is considered to be Gaussian [9], is given below

$$P(R_p|\boldsymbol{\eta}) \propto \exp\Big(-(R_p - R_{\boldsymbol{\eta}})^\top \Sigma (R_p - R_{\boldsymbol{\eta}})\Big), \tag{4}$$

where $R_{\boldsymbol{\eta}}$ represents the simulated pressure data. We constructed the covariance matrix Σ to be $\Sigma = \boldsymbol{I}/2\sigma_R^2$, where $\boldsymbol{I}$ is the identity matrix and σ_R^2 is the precision parameter associated with the measured pressure data.

To sample from the posterior distribution (3) the MCMC algorithm is used. The algorithm has an instrumental distribution $I(\boldsymbol{\eta}_p|\boldsymbol{\eta})$, where $\boldsymbol{\eta}$ is the previously accepted sample, and $\boldsymbol{\eta}_p = \boldsymbol{\eta}(\boldsymbol{\theta}_p)$ is proposed at each iteration. For a given permeability field, the forward problem is solved numerically to give $R_{\boldsymbol{\eta}}$. In the MCMC algorithm the acceptance probability is calculated as in [25]. The probability is given by

$$\alpha(\boldsymbol{\eta}, \boldsymbol{\eta}_p) = \min\left(1, \frac{I(\boldsymbol{\eta}|\boldsymbol{\eta}_p)P(\boldsymbol{\eta}_p|R_p)}{I(\boldsymbol{\eta}_p|\boldsymbol{\eta})P(\boldsymbol{\eta}|R_p)}\right). \tag{5}$$

3.2 Dimensional Reduction

In the MCMC algorithm, at each iteration we need a permeability value of each computational cell of the physical domain. This leads to a huge parameter space and the problem becomes impractical as the number of computational cells increases. In order to reduce the parameter space, we consider a Karhunen Loève expansion [12,21]. Here we briefly discuss the expansion.

For $\boldsymbol{x} \in \Omega$, let $\log[k(\boldsymbol{x})] = Y^k(\boldsymbol{x})$ to be a Gaussian field sample. In addition, we also assume that $Y^k(\boldsymbol{x}) \in L^2(\Omega)$ is a second order stochastic process with unit probability. The assumption $E[(Y^k)^2] = 0$ allows us to express the permeability field $Y^k(\boldsymbol{x})$ for a given orthonormal basis $\{\varphi_i\}$ of $L^2(\Omega)$ as follows:

$$Y^k(\boldsymbol{x}) = \sum_{i=1}^{\infty} Y_i^k \varphi_i(\boldsymbol{x}), \tag{6}$$

with random coefficients $Y_i^k = \int_\Omega Y^k(\boldsymbol{x})$. The eigenfunctions $\varphi_i(\boldsymbol{x})$ for the corresponding eigenvalues λ_i satisfy the integral equation

$$\int_\Omega R(\boldsymbol{x}_1, \boldsymbol{x}_2)\varphi_i(\boldsymbol{x}_2)d\boldsymbol{x}_2 = \lambda_i \varphi_i(\boldsymbol{x}_1), \quad i = 1, 2, \ldots \tag{7}$$

where $R(\boldsymbol{x}_1, \boldsymbol{x}_2)$ is a covariance function. Note that the eigenvalues are positive, i.e., $\lambda_i = E[(Y^k)^2] > 0$ and arranged in descending order. Using $\theta_i^k = Y_i^k/\sqrt{\lambda_i}$, Eq. (6) becomes

$$Y^k(\boldsymbol{x}) = \sum_{i=1}^{\infty} \sqrt{\lambda_i}\theta_i^k \varphi_i(\boldsymbol{x}), \tag{8}$$

where the pair (λ_i, φ_i) satisfy Eq. (7). The series written in the Eq. (8) is called KLE. To make sure that the energy E is above 95% [19] we need the first N dominating eigenvalues in KLE, i.e.,

$$E = \frac{\sum_{i=1}^{N} \lambda_i}{\sum_{i=1}^{\infty} \lambda_i} \geq 95\%. \tag{9}$$

We, therefore, calculate the truncated KLE by

$$Y_N^k(\boldsymbol{x}) = \sum_{i=1}^{N} \sqrt{\lambda_i}\theta_i^k \varphi_i(\boldsymbol{x}). \tag{10}$$

3.3 MCMC Convergence Assessment

In the MCMC algorithm we need to address two critical questions: (i) How do we pick an initial seed for an MCMC simulation? and (ii) What are the stopping criteria of an MCMC simulation? In the past the researchers in [27, 29,31] worked on establishing a theoretical approach for the stopping criteria. However, in practice, we often use empirical diagnostic tools, such as in [5,22, 24,30] to analyze the convergence of an MCMC algorithm. In this subsection, we consider two mostly used diagnostics namely the Potential Scale Reduction Factor (PSRF) and the multivariate PSRF (MPSRF). MPSRF is more reliable than PSRF for parallel chains because MPSRF takes all the parameters into account.

We choose l posterior draws from each of the m chains and a parameter vector $\boldsymbol{\theta}$ of dimension N. We consider $\boldsymbol{\theta}_j^c$ as the value of the vector $\boldsymbol{\theta}$ generated at iteration c in the jth chain of the MCMC algorithm. The pooled variance estimate $\widehat{\mathbf{V}}$ is calculated by the weighted average of the between ($\mathbf{B}$) and within chain variance estimates ($\mathbf{W}$) and is given by

$$\widehat{\mathbf{V}} = \frac{l-1}{l}\mathbf{W} + \left(1 + \frac{1}{m}\right)\frac{\mathbf{B}}{l}. \tag{11}$$

The covariance matrices are defined as

$$\mathbf{W} = \frac{1}{m(l-1)} \sum_{j=1}^{m} \sum_{c=1}^{l} \left(\boldsymbol{\theta}_j^c - \bar{\boldsymbol{\theta}}_{j.}\right)\left(\boldsymbol{\theta}_j^c - \bar{\boldsymbol{\theta}}_{j.}\right)^T, \tag{12}$$

and

$$\mathbf{B} = \frac{l}{m-1} \sum_{j=1}^{m} \left(\bar{\boldsymbol{\theta}}_{j.} - \bar{\boldsymbol{\theta}}_{..}\right)\left(\bar{\boldsymbol{\theta}}_{j.} - \bar{\boldsymbol{\theta}}_{..}\right)^T, \tag{13}$$

where $\bar{\boldsymbol{\theta}}_{j.}$ represents within chain mean and $\bar{\boldsymbol{\theta}}_{..}$ denotes the mean between m combined chains. The superscript T indicates the transpose of a matrix. The PSRFs are estimated as

$$\text{PSRF}_\text{i} = \sqrt{\frac{\text{diag}(\widehat{\mathbf{V}})_i}{\text{diag}(\mathbf{W})_i}}, \quad \text{where } i = 1, 2, ..., N. \tag{14}$$

If m chains start sampling from the stationary distribution, the estimators $\widehat{\mathbf{V}}$ and $\widehat{\mathbf{W}}$ should be very close to each other and thus the horizontal line drawn at 1

becomes a horizontal asymptote for the maximum of PSRF curves and indicates the convergence of the MCMC simulations. Using the maximum root statistic, as in [5] MPSRF is defined by

$$\begin{aligned}\text{MPSRF} &= \sqrt{\max_{\mathbf{a}} \frac{\mathbf{a}^T \widehat{\mathbf{V}} \mathbf{a}}{\mathbf{a}^T \mathbf{W} \mathbf{a}}} \\ &= \sqrt{\max_{\mathbf{a}} \frac{\mathbf{a}^T \left[\frac{l-1}{l}\mathbf{W} + \left(1+\frac{1}{m}\right)\frac{\mathbf{B}}{l}\right]\mathbf{a}}{\mathbf{a}^T \mathbf{W} \mathbf{a}}} \\ &= \sqrt{\frac{l-1}{l} + \left(\frac{m+1}{m}\right) \max_{\mathbf{a}} \frac{\mathbf{a}^T \frac{\mathbf{B}}{l} \mathbf{a}}{\mathbf{a}^T \mathbf{W} \mathbf{a}}} \\ &= \sqrt{\frac{l-1}{l} + \left(\frac{m+1}{m}\right) \lambda},\end{aligned}$$

where $\mathbf{a} \in \mathbb{R}^N$ is an arbitrary vector and λ is the largest eigenvalue of the matrix $\mathbf{W}^{-1}\mathbf{B}/l$. The equality in means of between chains makes the covariance matrix $\mathbf{B}$ zero and eventually MPSRF approaches 1 and thus indicates the convergence of the MCMC simulations.

4 Multiscale Maximum Change Algorithm

4.1 The Multiscale Prior Distribution

The Multiscale Maximum Change strategy consists of two non-overlapping partitions of the domain Ω: the first one is a uniform fine Cartesian mesh Ω^f and the other one is a coarse Cartesian mesh Ω^c. The coarse mesh Ω^c is constructed as a set of elements of Ω^f (see Fig. 1) in which we use the values of the absolute permeability field as piecewise constant. We use KLE for the local dimensional reduction. Let Ω^γ be a partitions into rectangles $\{\Omega_i^\gamma,\ i = 1, \ldots, M_\gamma\}$, such that

$$\overline{\Omega^\gamma} = \bigcup_{i=1}^{M_\gamma} \overline{\Omega_i^\gamma}; \quad \Omega_i^\gamma \cap \Omega_k^\gamma = \varnothing, \quad i \neq k, \quad \gamma = c, f.$$

Define $\Gamma = \partial\Omega$ and, for $i = 1, \ldots, M_\gamma$:

$$\Gamma_{ik}^\gamma = \Gamma_{ki}^\gamma = \partial\Omega_i^\gamma \cap \partial\Omega_k^\gamma, \quad \gamma = c, f.$$

For the coarse partition $\{\Omega_i^\gamma,\ i = 1, \ldots, M_c\}$ elements, we define the set

$$\mathcal{S}_i = \{j : \Omega_j^f \subset \Omega_i^c\}.$$

We apply two length scales in the description of the new multiscale procedure: H and h for the coarse and the underlying fine grid mesh size, respectively. We decompose the vector $\boldsymbol{\theta}$ in Eq. (10) by using random walk sampler (RWS) [17]:

$$\boldsymbol{\theta}_p = \sqrt{1-\beta^2}\,\boldsymbol{\theta} + \beta\,\boldsymbol{\varepsilon}, \tag{15}$$

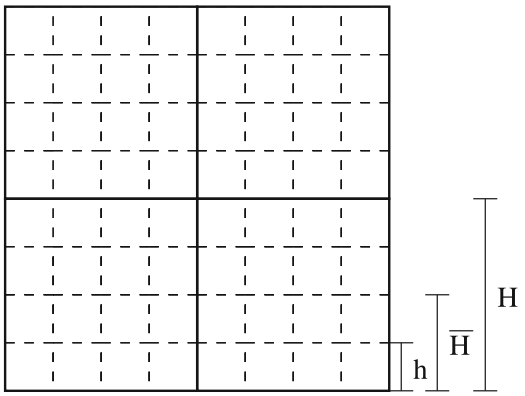

Fig. 1. The coarse Ω^c and fine Ω^f partitions of Ω represented by solid and dashed lines respectively along with three spatial scales.

where $\boldsymbol{\theta}_p$ and $\boldsymbol{\theta}$ are respectively the current and the previously accepted sample, β is used for tuning the sampler and $\boldsymbol{\varepsilon} \in \mathcal{N}(0, 1)$.

The samples produced in this approach are Gaussian samples with discontinuities in Γ^c_{ik}. To remove the flux discontinuities at boundaries, downscaling strategies have been developed for multiscale methods [17]. Inspired by the strategies, we complete the construction of a sample from our multiscale prior distribution by using an averaging method. The method is used to condition each sample on the available data at nearest neighbor subdomains [4]. The method is illustrated in Fig. 2.

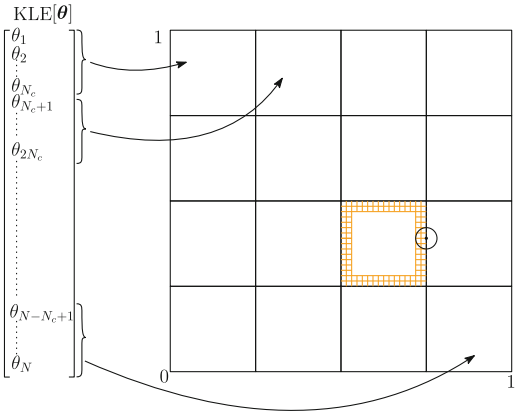

Fig. 2. Correspondence between blocks of theta variables and elements of the coarse partition Ω^c (solid lines) of Ω. Each block of thetas generates a localized Gaussian field in its corresponding subdomain.

A length scale $\overline{H}$ smaller than H is set and, for each i, all the current values of the cells of $\mathcal{S}_i$ are replaced by the local averages (that preserves mean and

variance for uncorrelated data). Note that the replacement is done based on the distance of $\overline{H}$ (or less) to Γ_{ik}^{c}. A sample before and after this averaging procedure is depicted in Fig. 3. The circle for the averaging shown in Fig. 2 is replaced by an ellipse if the correlation lengths are unequal. The averaging is applied on the top right subdomain boundary using $H = 0.25$. The multiscale prior distribution needs two parameters H and $\overline{H}$ from the user.

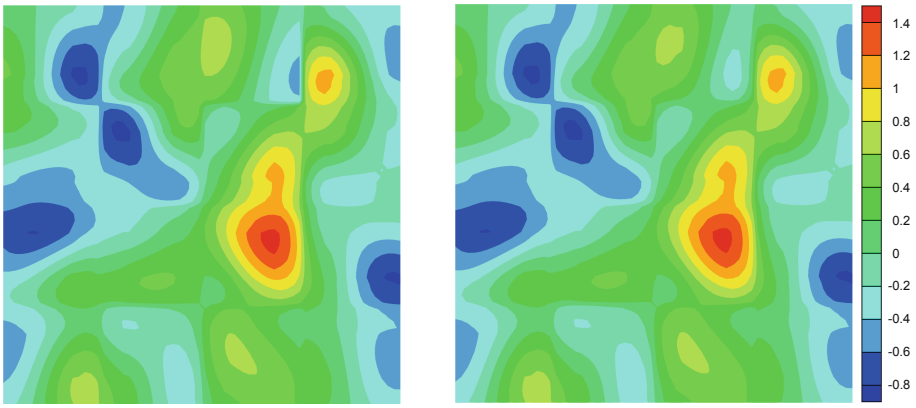

Fig. 3. Permeability field sample before (left) and after (right) local averaging is implemented on the top right subdomain of a domain decomposition with $H = 0.25$.

We define the local stochastic dimension to be $N_c = N/M_c$ and L to be the largest correlation length of the prior distribution. For $L < H$, it is expected that an improved convergence for MCMCs should be observed [4].

4.2 The Multiscale Sampling Method

When the number of subdomains $M_c = 1$, the MSM algorithm reduces to the classic preconditioned MCMC [6,9].

Let us first discuss the preconditioned MCMC algorithm. The preconditioned MCMC algorithm requires a coarse-scale model approximation to the pressure-velocity equation Eq. (1). This approximation is the basis for the filtering step of this method. The discretization for both scales, coarse and fine, is similar to each other. An upscaling procedure [8] is applied to produce effective permeability field. The coarse-grid pressure field R_c is calculated by running the numerical simulator on the coarse-scale grid. The coarse-scale acceptance probability α_c and fine-scale acceptance probability α_f are defined by

$$\begin{aligned} \alpha_c(\boldsymbol{\eta}, \boldsymbol{\eta}_p) &= \min\left(1, \frac{I(\boldsymbol{\eta}|\boldsymbol{\eta}_p) P_c(\boldsymbol{\eta}_p|R_p)}{I(\boldsymbol{\eta}_p|\boldsymbol{\eta}) P_c(\boldsymbol{\eta}|R_p)}\right), \text{ and} \\ \alpha_f(\boldsymbol{\eta}, \boldsymbol{\eta}_p) &= \min\left(1, \frac{P_f(\boldsymbol{\eta}_p|R_p) P_c(\boldsymbol{\eta}|R_p)}{P_f(\boldsymbol{\eta}|R_p) P_c(\boldsymbol{\eta}_p|R_p)}\right), \end{aligned} \tag{16}$$

respectively, where P_c and P_f refer to the posterior probabilities calculated at coarse-scale and fine-scale, respectively. In MSM, the global permeability field is constructed by taking the local averages. The local permeability field $\boldsymbol{\eta}(\boldsymbol{\theta}^i)$ for each subdomain $\Omega_i^c, i = 1, \ldots M_c$ is constructed by generating local KLE using Eq. (10).

4.3 The Multiscale Maximum Change Method

The Multiscale Maximum Change Method (MMCM) consists of two steps namely the screening and local search steps. In the first step, we complete a certain number of iterations (N number of iterations) and update all the stochastic parameters of the vector $\boldsymbol{\theta}$. Next, we pick a specific subdomain (the winner subdomain) among all the subdomains M_c and localize the search to better explore the posterior distribution. We choose the winner subdomain ($M_i, i \leq c$) in such a way that the likelihood function in Eq. (4) is minimized. That means the subdomain that gives maximum change, i.e., $|E_i - E_{i-1}|$ is the maximum, where E_i and E_{i-1} are the errors of the last accepted proposal in the subdomains i and $i-1$, respectively. The algorithm for MMCM is presented in Algorithm 1.

Algorithm 1. The Multiscale Maximum Change Method (MMCM)

1: For all the subdomains, $\Omega_i^c, i = 1, \ldots, M_c$, solve Eq. (7) to get a KLE in Eq. (10) by using a given covariance function R.
2: **for** $j = 1$ to M_{mcmc} **do**
3: **for** $i = 1$ to M_c **do**
4: **for** $k = 1$ to N_c **do**
5: Generate Gaussian variables i.i.d., $\mathcal{N}(0, 1)$ to construct $\boldsymbol{\theta}_p$ using Eq. (15) in Ω_i^c.
6: The Gaussian preliminary value sample at the $\mathcal{S}_i$ cells are constructed by a local Gaussian sample using the KLE.
7: Remove discontinuities by using the averaging method.
8: Estimate the upscaled permeability on the coarse-scale using $\boldsymbol{\eta}_p$.
9: Solve the forward problem on the coarse-scale to get R_c.
10: Calculate the acceptance probability $\alpha_c(\boldsymbol{\eta}, \boldsymbol{\eta}_p)$.
11: **if** $\boldsymbol{\eta}_p$ is accepted **then**
12: Use $\boldsymbol{\eta}_p$ to get R_f.
13: Compute the acceptance probability $\alpha_f(\boldsymbol{\eta}, \boldsymbol{\eta}_p)$.
14: **if** $\boldsymbol{\eta}_p$ is accepted **then** $\boldsymbol{\eta} = \boldsymbol{\eta}_p$.
15: **end if**
16: **end if**
17: $j = j + 1$.
18: **end for**
19: **end for**
20: Pick the winner subdomain by using the winning criterion.
21: Continue with the steps from 5-17 for $2 \times N_c$ times.
22: **end for**

5 Numerical Results

In this section we discuss the MCMC simulations using MSM and MMCM. The pressure-velocity equation Eq. (1) is numerically solved on the domain $\Omega = [0,1] \times [0,1]$. The numerical simulator is run repeatedly in the MCMC algorithm on a GPU cluster. At each iteration in the MCMC simulation, the numerical simulator needs the distribution of permeability values on the physical domain. For that we first construct a permeability field for each subdomain by applying KLE and then the global permeability field is constructed. In KLE, we define the covariance function as follows:

$$R(\boldsymbol{x}_1, \boldsymbol{x}_2) = \sigma_Y^2 \exp\left(-\frac{|x_1 - x_2|^2}{2L_x^2} - \frac{|y_1 - y_2|^2}{2L_y^2}\right), \tag{17}$$

where L_x and L_y are the correlation lengths. We take $L_x = L_y = 0.2$ and $\sigma_Y^2 = \mathrm{Var}[(Y^k)^2] = 1$. Moreover, we set a zero source term and impose Dirichlet boundary conditions $p = 1$ on the left and $p = 0$ on the right boundaries. No-flow (Neumann-type boundary condition) condition is set on the top and bottom boundaries.

We generate a KLE in each of MSM and MMCM. In both methods, we use $H = 0.5$. The first 20 eigenvalues preserving 97% of the total energy are chosen, and five eigenvalues are chosen for each subdomain. Figure 4 shows the decay of the eigenvalues. We run four MCMCs in parallel for each method.

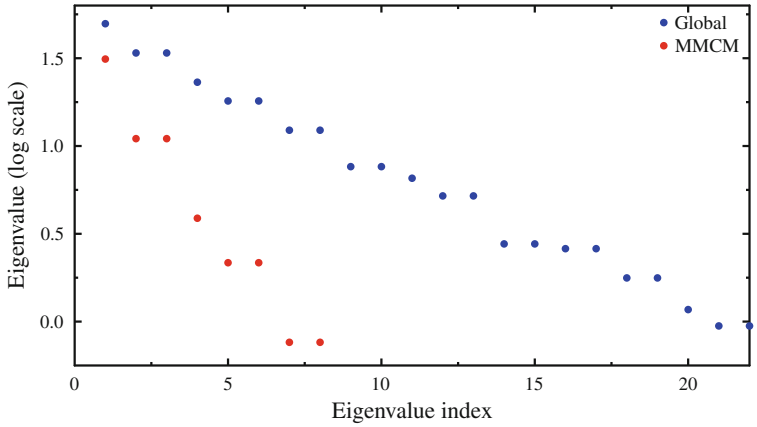

Fig. 4. The decay of the global and local eigenvalues.

On our computational domain of size 16×16 (fine-grid), we generate a reference synthetic permeability field. We then run the GPU numerical simulator [13,14] to generate the pressure field corresponding to this reference permeability field. The pressure values at alternate cells (similar to the black squares of a chessboard) are referred to as pressure measurements. The reference permeability field and the corresponding pressure values are shown in Fig. 5.

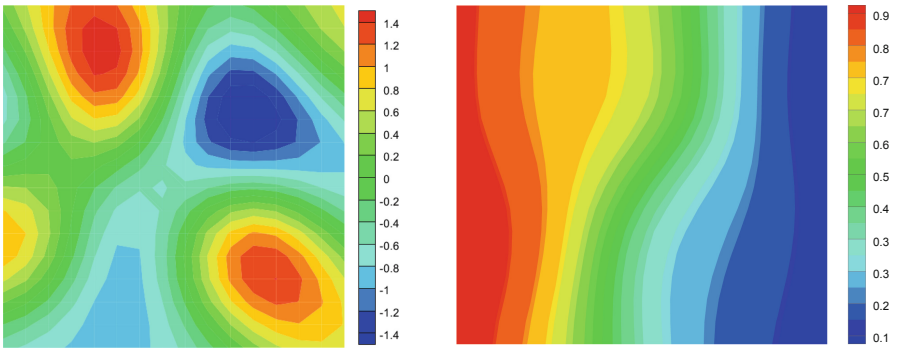

Fig. 5. Reference log permeability field (left) and the corresponding reference pressure field (right).

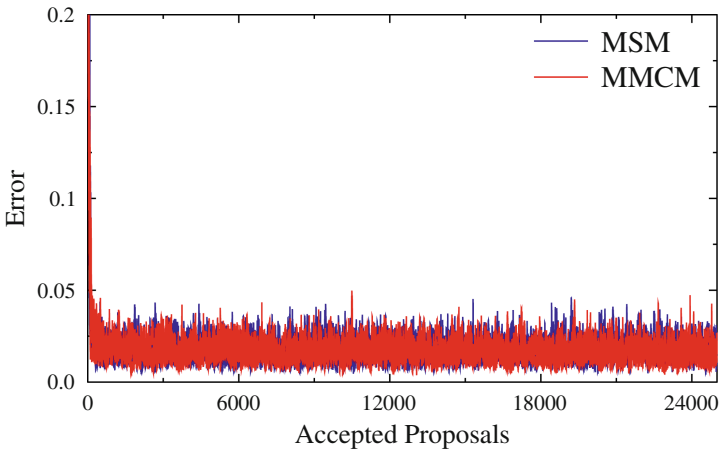

Fig. 6. Error curves of the MSM and MMCM.

We use the maximum of PSRFs and MPSRF to examine the convergence of the MCMC simulations as discussed in Subsect. refmpsrfsps3. If both the MPSRF value and the maximum value of PSRFs approach 1.2, an MCMC simulation can be considered converged to the stationary distribution [32]. Figure 7 shows that both preconditioned MCMC algorithms (MSM and MMCM) converged. The MMCM simulation, however, converges to the stationary distribution faster than

the MSM as shown by the bottom plots of Fig. 7. Figure 6 displays the errors for both algorithms. The error at each iteration is calculated by the absolute value of the difference between the reference and simulated pressure data.

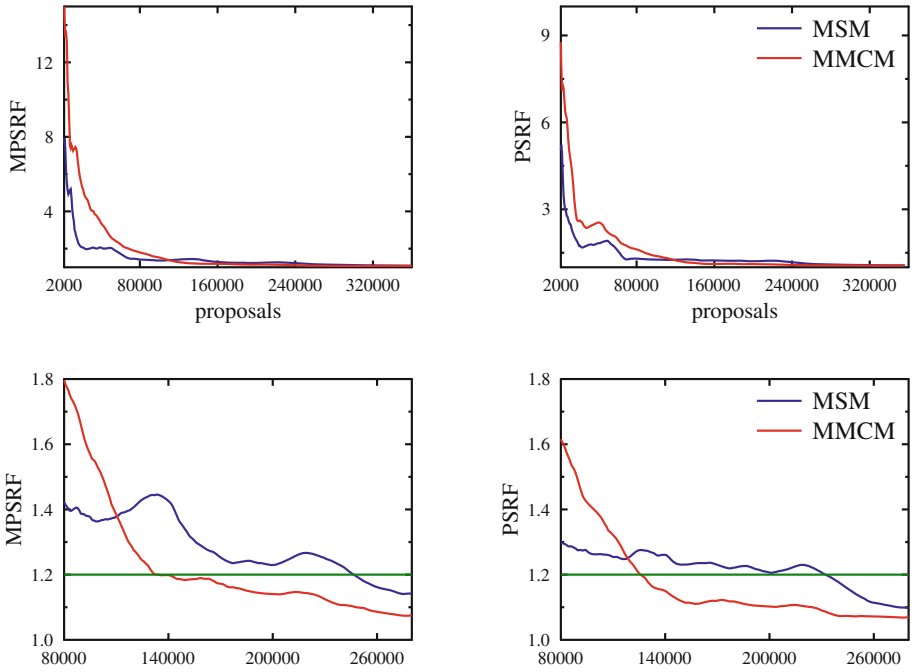

Fig. 7. Top: The maximum of MPSRF and PSRFs for the MSM and MMCM method. Bottom: Tails of the maximum of MPSRF and PSRFs curves.

Figure 8 and Fig. 9 show the accepted permeability fields in two sets of MCMC simulations. The permeability fields generated by MMCM resemble closer to the reference permeability field than those of MSM despite the fact that both methods converged. A similar behavior was observed in other MCMC simulations, as well.

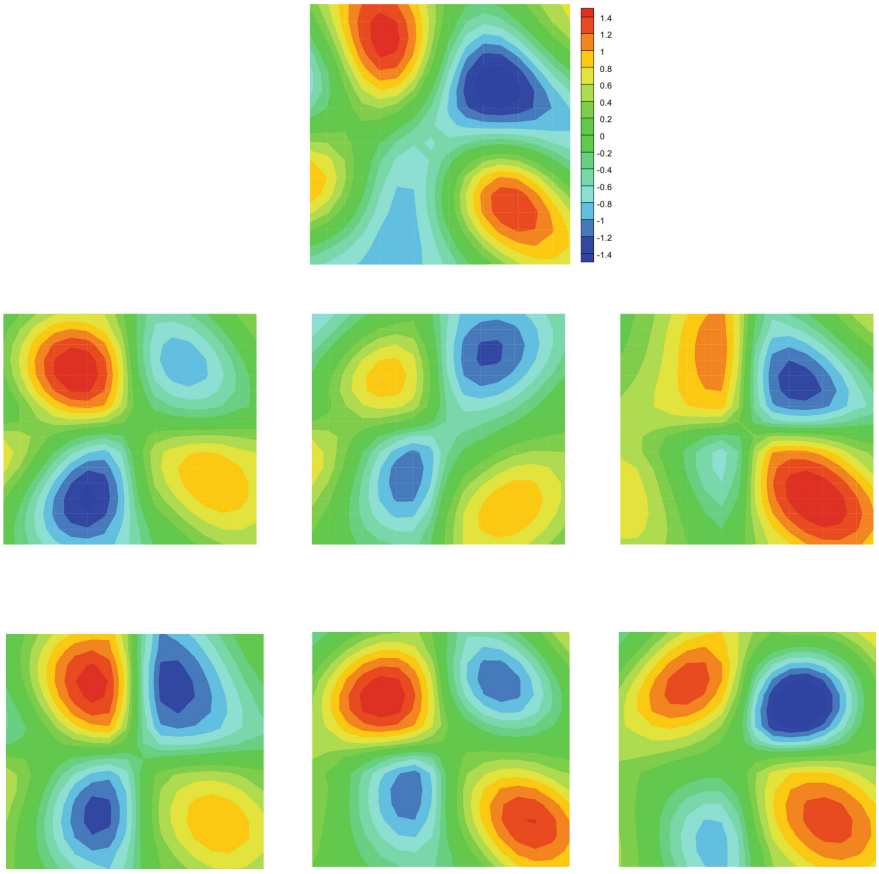

Fig. 8. First row: Reference log permeability filed. Second row: Accepted permeability fields in MSM. Third row: Accepted permeability fields in MMCM. From left to right, log permeability fields at 20000, 40000 and 60000 iterations, respectively, from a set of chains.

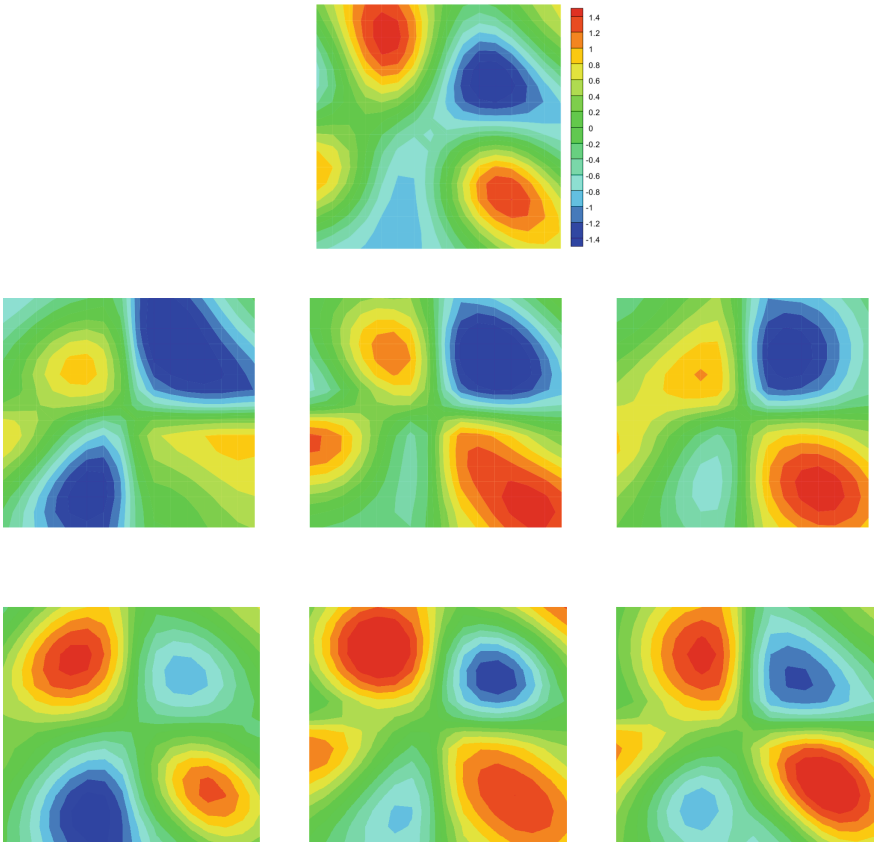

Fig. 9. First row: Reference log permeability filed. Second row: Accepted permeability fields in MSM. Third row: Accepted permeability fields in MMCM. From left to right, log permeability fields at 20000, 40000 and 60000 iterations, respectively, from another set of chains.

6 Conclusions

In this paper we considered the permeability characterization of an aquifer conditioned on measured pressure data. A Bayesian framework was used for the characterization. To improve the convergence rate of the MCMC algorithm in the framework, the new Multiscale Maximum Change Method was introduced. This method is an improvement of the Multiscale Sampling Method. MMCM consists of two steps. In the screening step, we complete a fixed number of iterations on each subdomain and update all the parameters in the stochastic space. In the local search step, we pick the winner subdomain and localize the search to better explore the posterior distribution. The numerical simulations show that both MSM and MMCM converge, but MMCM shows improved convergence.

Acknowledgements. A. Rahunanthan research was supported by NIFA/USDA through Central State University's Evans-Allen Research Program.

All the numerical simulations presented in this paper were performed on the GPU Computing cluster housed in the Department of Mathematics and Computer Science at Central State University.

References

1. Akbarabadi, M., Borges, M., Jan, A., Pereira, F., Piri, M.: A Bayesian framework for the validation of models for subsurface flows: synthetic experiments. Comput. Geosci. **19**(6), 1231–1250 (2015). https://doi.org/10.1007/s10596-015-9538-z
2. Al-Mamun, A., Barber, J., Ginting, V., Pereira, F., Rahunanthan, A.: Contaminant transport forecasting in the subsurface using a Bayesian framework. Appl. Math. Comput. **387**, 124980 (2020)
3. Ali, A., Al-Mamun, A., Pereira, F., Rahunanthan, A.: Multiscale sampling for the inverse modeling of partial differential equations (2023). https://doi.org/10.48550/ARXIV.2302.11149
4. Ali, A.A.H.: Multiscale Sampling for Subsurface Characterization. The University of Texas at Dallas (2021)
5. Brooks, S., Gelman, A.: General methods for monitoring convergence of iterative simulations. J. Comput. Graph. Stat. **7**, 434–455 (1998)
6. Christen, J.A., Fox, C.: Markov chain Monte Carlo using an approximation. J. Comput. Graph. Stat. **14**(4), 795–810 (2005)
7. Contreras, A.A., Mycek, P., Maítre, O.P., Rizzi, F., Debusschere, B., Knio, O.M.: Parallel domain decomposition strategies for stochastic elliptic equations. part a: local Karhunen-Loève representations. SIAM J. Sci. Statist. Comput. **40**(4), C520–C546 (2018)
8. Durlofsky, L.: Numerical calculation of equivalent grid block permeability tensors for heterogeneous porous media. Water Resour. Res. **27**(5), 699–708 (1991)
9. Efendiev, Y., Hou, T., Luo, W.: Preconditioning Markov chain Monte Carlo simulations using coarse-scale models. SIAM J. Sci. Comput. **28**, 776–803 (2006)
10. Francisco, A., Ginting, V., Pereira, F., Rigelo, J.: Design and implementation of a multiscale mixed method based on a nonoverlapping domain decomposition procedure. Math. Comput. Simul. **99**, 125–138 (2014)
11. Ginting, V., Pereira, F., Rahunanthan, A.: Multiple Markov chains Monte Carlo approach for flow forecasting in porous media. Procedia Comput. Sci. **9**, 707–716 (2012)
12. Ginting, V., Pereira, F., Rahunanthan, A.: A multi-stage Bayesian prediction framework for subsurface flows. Int. J. Uncertain. Quantif. **3**(6), 499–522 (2013)
13. Ginting, V., Pereira, F., Rahunanthan, A.: A prefetching technique for prediction of porous media flows. Comput. Geosci. **18**(5), 661–675 (2014). https://doi.org/10.1007/s10596-014-9413-3
14. Ginting, V., Pereira, F., Rahunanthan, A.: Rapid quantification of uncertainty in permeability and porosity of oil reservoirs for enabling predictive simulation. Math. Comput. Simul. **99**, 139–152 (2014)
15. Ginting, V., Pereira, F., Rahunanthan, A.: Multi-physics Markov chain Monte Carlo methods for subsurface flows. Math. Comput. Simul. **118**, 224–238 (2015)
16. Guiraldello, R.T., Ausas, R.F., Sousa, F.S., Pereira, F., Buscaglia, G.C.: The multiscale Robin coupled method for flows in porous media. J. Comput. Phys. **355**, 1–21 (2018)

17. Guiraldello, R.T., Ausas, R.F., Sousa, F.S., Pereira, F., Buscaglia, G.C.: Velocity postprocessing schemes for multiscale mixed methods applied to contaminant transport in subsurface flows. Comput. Geosci. **24**(3), 1141–1161 (2020). https://doi.org/10.1007/s10596-019-09930-8
18. Jaramillo, A., et al.: Towards HPC simulations of billion-cell reservoirs by multiscale mixed methods. arXiv preprint arXiv:2103.08513 (2021)
19. Laloy, E., Rogiers, B., Vrugt, J., Mallants, D., Jacques, D.: Efficient posterior exploration of a high-dimensional groundwater model from two-stage Markov chain Monte Marlo simulation and polynomial chaos expansion. Water Resour. **49**(5), 2664–2682 (2013)
20. Liao, Q., Willcox, K.: A domain decomposition approach for uncertainty analysis. SIAM J. Sci. Comput. **37**(1), A103–A133 (2015)
21. Loève, M.: Probability Theory. Springer, Berlin (1997)
22. Cowles, M.K., Carlin, B.P.: Markov chain Monte Carlo convergence diagnostics: a comparative review. J. Am. Stat. Assoc. **91**, 883–904 (1996)
23. Mamun, A., Pereira, F., Rahunanthan, A.: Convergence analysis of MCMC methods for subsurface flow problems. In: Gervasi, O., et al. (eds.) ICCSA 2018. LNCS, vol. 10961, pp. 305–317. Springer, Cham (2018). https://doi.org/10.1007/978-3-319-95165-2_22
24. Mengersen, K.L., Robert, C.P., Guihenneuc-Jouyaux, C.: MCMC convergence diagnostics: a review. In: Bernardo, M., Berger, J.O., Dawid, A.P., Smtith, A.F.M. (eds.) Bayesian Statistics, vol. 6, pp. 415–440. Oxford University Press (1999)
25. Metropolis, N., Ulam, S.: The Monte Carlo method. J. Am. Stat. Assoc. **44**(247), 335–341 (1949)
26. Pereira, F., Rahunanthan, A.: A semi-discrete central scheme for the approximation of two-phase flows in three space dimensions. Math. Comput. Simul. **81**(10), 2296–2306 (2011)
27. Polson, N.G.: Convergence of Markov chain Monte Carlo algorithms. In: Bernardo, J.M., Berger, J.O., Dawid, A.P., Smith, A.F.M. (eds.) Bayesian Statistics, vol. 5, pp. 297–322 (1996)
28. Quarteroni, A.M., Valli, A.: Domain Decomposition Methods for Partial Differential Equations. Oxford University Press, Oxford (1999)
29. Rosenthal, J.S.: Minorization conditions and convergence rates for Markov chain Monte Carlo. J. Am. Stat. Assoc. **90**(430), 558–566 (1995)
30. Roy, V.: Convergence diagnostics for Markov chain Monte Carlo. Annu. Rev. Stat. Appl. **7**, 387–412 (2019)
31. Brooks, S.P., Roberts, G.O.: Convergence assessment techniques for Markov chain Monte Carlo. Stat. Comput. **8**, 319–335 (1998)
32. Smith, B.J.: boa: an R package for MCMC output convergence assessment and posterior inference. J. Stat. Softw. **21**, 1–37 (2007)
33. Stuart, G.K., Minkoff, S.E., Pereira, F.: A two-stage Markov chain Monte Carlo method for seismic inversion and uncertainty quantification. Geophysics **84**(6), R1003–R1020 (2019)
34. Tong, X.T., Morzfeld, M., Marzouk, Y.M.: MALA-within-Gibbs samplers for high-dimensional distributions with sparse conditional structure. SIAM J. Sci. Comput. **42**(3), A1765–A1788 (2020)